Article

Structures and Displacement of 1-Adamantanethiol Self-Assembled Monolayers on Au{111}

Arrelaine A. Dameron, Lyndon F. Charles, and Paul S. Weiss

J. Am. Chem. Soc., **2005**, 127 (24), 8697-8704• DOI: 10.1021/ja042621o • Publication Date (Web): 24 May 2005

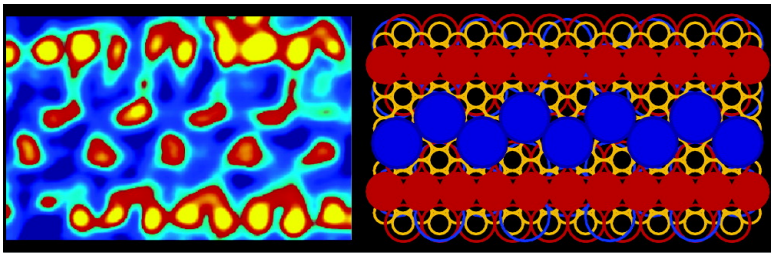

J|A|C|S
ARTICLES
Published on Web 05/24/2005

Structures and Displacement of 1-Adamantanethiol Self-Assembled Monolayers on Au{111}

Arrelaine A. Dameron, Lyndon F. Charles, and Paul S. Weiss*

Contribution from the Departments of Chemistry and Physics, The Pennsylvania State University, University Park, Pennsylvania 16802-6300

Received December 8, 2004; E-mail: stm@psu.edu

Abstract: We have designed monolayers with weak intermolecular interactions for use as placeholders in intelligent self- and directed-assembly. We have shown that these 1-adamantanethiolate monolayers are labile with respect to displacement by exposing them to dilute solutions of alkanethiols. These self-assembled monolayers (SAMs) of 1-adamantanethiol on Au{111} were probed using ambient scanning tunneling microscopy (STM), and their assembled order was determined. Solution deposition of the molecules results in a highly ordered hexagonally close-packed molecular lattice with a measured nearest neighbor distance of 6.9 ± 0.4 Å. The SAMs exhibit several rotational domains, but lack the protruding domain boundaries typical of alkanethiolate SAMs, and are similarly stable at room temperature. Co-deposition of alkanethiol and 1-adamantanethiol from solution results in alkanethiolate SAMs, except when using extremely low alkanethiol to 1-adamantanethiol concentration ratios. Facile displacement of low interaction strength SAMs can be exploited to enhance patterning using soft nanolithography.

1. Introduction

In the field of nanoscale fabrication, self-assembly techniques are being rapidly developed as device structures are getting smaller and more intricate. Self-assembly is especially appealing because of the ease of manufacture and the variety of applicable systems. As such, self-assembled monolayers (SAMs) have been extensively studied for use as matrices for molecular components,[1−8] media for patterning,[5,9−119−11] and simple models for organic thin films.[9,12−21] For self-assembled systems, tuning the chemical and physical properties of the assembled molecules can result in control of the chemical and physical properties of the entire system, an attribute that is sought for molecular devices.[11,22,23,] It is useful to have a library of molecules that form SAMs with distinctive properties so that in the future it is possible to create monolayers that are uniquely designed for their application. This can be achieved by tuning the molecular topology and the intermolecular interactions within the SAMs.

The most rigorously characterized SAMs to date are alkanethiolate SAMs on Au{111}.[16,24−29] Alkanethiolate SAMs are fabricated easily from thiols or disulfides via a variety of methods because they form spontaneously on Au{111} by chemisorption of the sulfur headgroup to the gold surface. These SAMs are well ordered and highly stable because of two properties: the strong sulfur−gold bond, and the attractive van der Waals forces between adjacent alkyl chains.[13,20,28,30,31] These

(1) Bumm, L. A.; Arnold, J. J.; Cygan, M. T.; Dunbar, T. D.; Burgin, T. P.; Jones, L.; Allara, D. L.; Tour, J. M.; Weiss, P. S. *Science* **1996**, *271*, 1705.
(2) Bumm, L. A.; Arnold, J. J.; Dunbar, T. D.; Allara, D. L.; Weiss, P. S. *J. Phys. Chem. B* **1999**, *103*, 8122.
(3) Donhauser, Z. J.; Mantooth, B. A.; Kelly, K. F.; Bumm, L. A.; Monnell, J. D.; Stapleton, J. J.; Price, D. W.; Rawlett, A. M.; Allara, D. L.; Tour, J. M.; Weiss, P. S. *Science* **2001**, *292*, 2303.
(4) Donhauser, Z. J.; Mantooth, B. A.; Pearl, T. P.; Kelly, K. F.; Nanayakkara, S. U.; Weiss, P. S. *Jpn. J. Appl. Phys., Part 1* **2002**, *41*, 4871.
(5) Lewis, P. A.; Donhauser, Z. J.; Mantooth, B. A.; Smith, R. K.; Bumm, L. A.; Kelly, K. F.; Weiss, P. S. *Nanotechnology* **2001**, *12*, 231.
(6) Stapleton, J. J.; Harder, P.; Daniel, T. A.; Reinard, M. D.; Yao, Y. X.; Price, D. W.; Tour, J. M.; Allara, D. L. *Langmuir* **2003**, *19*, 8245.
(7) Tour, J. M.; Jones, L.; Pearson, D. L.; Lamba, J. J. S.; Burgin, T. P.; Whitesides, G. M.; Allara, D. L.; Parikh, A. N.; Atre, S. V. *J. Am. Chem. Soc.* **1995**, *117*, 9529.
(8) Walzer, K.; Marx, E.; Greenham, N. C.; Less, R. J.; Raithby, P. R.; Stokbro, K. *J. Am. Chem. Soc.* **2004**, *126*, 1229.
(9) Bumm, L. A.; Arnold, J. J.; Charles, L. F.; Dunbar, T. D.; Allara, D. L.; Weiss, P. S. *J. Am. Chem. Soc.* **1999**, *121*, 8017.
(10) Smith, R. K.; Lewis, P. A.; Weiss, P. S. *Prog. Surf. Sci.* **2004**, *75*, 1.
(11) Smith, R. K.; Reed, S. M.; Lewis, P. A.; Monnell, J. D.; Clegg, R. S.; Kelly, K. F.; Bumm, L. A.; Hutchison, J. E.; Weiss, P. S. *J. Phys. Chem. B* **2001**, *105*, 1119.
(12) Dubois, L. H.; Nuzzo, R. G. *Annu. Rev. Phys. Chem.* **1992**, *43*, 437.
(13) Dubois, L. H.; Zegarski, B. R.; Nuzzo, R. G. *J. Vac. Sci. Technol. A* **1987**, *5*, 634.
(14) Laibinis, P. E.; Nuzzo, R. G.; Whitesides, G. M. *J. Phys. Chem.* **1992**, *96*, 5097.
(15) Nuzzo, R. G.; Zegarski, B. R.; Dubois, L. H. *J. Am. Chem. Soc.* **1987**, *109*, 733.
(16) Ogawa, H.; Takamura, T.; Shimoyama, Y. *Jpn. J. Appl. Phys., Part 1* **1999**, *38*, 6019.
(17) Poirier, G. E. *Chem. Rev.* **1997**, *97*, 1117.
(18) Poirier, G. E.; Tarlov, M. J.; Rushmeier, H. E. *Langmuir* **1994**, *10*, 3383.
(19) Poirier, G. E.; Tarlov, M. J. *Langmuir* **1994**, *10*, 2853.
(20) Ulman, A. *Chem. Rev.* **1996**, *96*, 1533.
(21) Ulman, A.; Eilers, J. E.; Tillman, N. *Langmuir* **1989**, *5*, 1147.
(22) Evans, S. D.; Urankar, E.; Ulman, A.; Ferris, N. *J. Am. Chem. Soc.* **1991**, *113*, 4121.
(23) Lewis, P. A.; Smith, R. K.; Kelly, K. F.; Bumm, L. A.; Reed, S. M.; Clegg, R. S.; Gunderson, J. D.; Hutchison, J. E.; Weiss, P. S. *J. Phys. Chem. B* **2001**, *105*, 10630.
(24) Edinger, K.; Golzhauser, A.; Demota, K.; Woll, C.; Grunze, M. *Langmuir* **1993**, *9*, 4.
(25) Kobayashi, K.; Yamada, H.; Horiuchi, T.; Matsushige, K. *Jpn. J. Appl. Phys., Part 1* **1998**, *37*, 6183.
(26) Noh, J.; Araki, T.; Nakajima, K.; Hara, M. *Mol. Cryst. Liq. Cryst.* **2001**, *371*, 95.
(27) Nuzzo, R. G.; Korenic, E. M.; Dubois, L. H. *J. Chem. Phys.* **1990**, *93*, 767.
(28) Poirier, G. E.; Pylant, E. D. *Science* **1996**, *272*, 1145.
(29) Ulman, A.; Evans, S. D.; Snyder, R. G. *Thin Solid Films* **1992**, *210*, 806.
(30) Barrena, E.; Palacios-Lidon, E.; Munuera, C.; Torrelles, X.; Ferrer, S.; Jonas, U.; Salmeron, M.; Ocal, C. *J. Am. Chem. Soc.* **2004**, *126*, 385.
(31) Delamarche, E.; Michel, B. *Thin Solid Films* **1996**, *273*, 54.

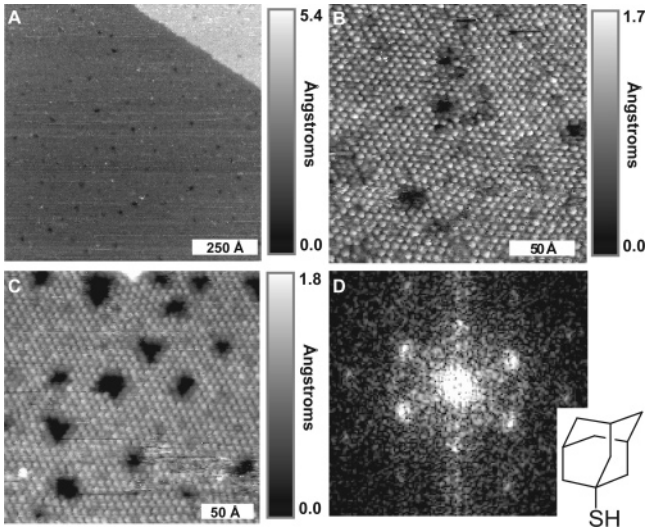

Figure 1. Scanning tunneling microscopy images showing the well-ordered hexagonal close-packed lattice of 1-adamantanethiolate self-assembled monolayers on Au{111}: (A) 1500 Å × 1500 Å, sample bias 0.75 V, current 6.0 pA; (B) 200 Å × 200 Å, sample bias 1.0 V, current 5.0 pA; (C) 250 Å × 250 Å, sample bias 750 mV, current 3.0 pA; (D) Fourier transform of C showing first-order and a few second-order reciprocal lattice points. The structure of 1-adamantanethiolate is given in the lower right corner for reference.

SAMs pack into a $(\sqrt{3} \times \sqrt{3})R30°$ geometry (with a nearest neighbor distance of 5.0 Å) with respect to the underlying Au{111} lattice and related superstructures, and they form large domains comprised of molecules with identical rotations and tilts. The boundaries separating the domains are discrete and often contain molecules protruding out of the SAM.[17,32] However, because of the prominent defects of alkanethiolate SAMs, such as tilt boundaries, rotational boundaries, and stacking faults,[17,19] they are not always completely reproducible matrices for device fabrication or patterned interfaces. Although some defects are inherent to the formation of thiolated SAMs on gold, with the correct choice of molecule, it should be possible to create a SAM with few domains and indistinct domain boundaries lacking significant defects.[33−35]

As a member of the diamondoid family, with the space group $F\bar{4}3m$, adamantane forms highly crystalline three-dimensional structures and is the subject of many crystallography and theory papers.[36−38] The molecule is comprised of a 10-carbon cage made of four fused cyclohexane rings in chair conformations.[39] Thus, each carbon is tetrahedrally sp^3-hybridized, and there is limited strain because each carbon−carbon bond is staggered.[38,40,41] The addition of a sulfur group, creating 1-adamantanethiol (see Figure 1), allows the carbon cage to be tethered to a gold surface while still keeping its round topology.[33,42,43] Structures similar to 1-adamantanethiol, such as bis(bicyclo[2,2,2]-octylmethyl)disulfide) and bis(tricyclo[3,3,1,1]decylmethyl)disulfide, have been assembled on Au{111} and studied by STM.[44,45] The two possible unit cells assigned to the SAMs of the latter, which differs from 1-adamantanethiol by an additional methylene unit between the adamantane cage and the sulfur atom, are $(4\sqrt{3} \times 4\sqrt{3})R30°$ and (7×7). Here, we utilize STM in ambient conditions to demonstrate that 1-adamantanethiol forms flat, highly ordered hexagonal close-packed, one-molecule-thick films on Au{111}. We show that 1-adamantanethiolate SAMs are labile with respect to displacement, which may make them useful as temporary protective layers in device fabrication or as placeholders, creating a means to hold useful molecules or molecular devices in place without the risk of disrupting their functionality.

2. Experimental Methods

2.1. 1-Adamantanethiol Synthesis. 1-Adamantanethiol was synthesized based on previously reported methods.[33,42,43,46,] In a three-neck flask, 10.7 g of 1-bromoadamantane (Aldrich), 50 mL of glacial acetic acid, 7.6 g of thiourea (Aldrich), and 25 mL of 48% HBr were refluxed for more than 3 h under argon. Formation of the 1-adamantyl isothiuronium salt was monitored with thin-layer chromatography, and after refluxing, the solution was allowed to cool to room temperature overnight. The salt was filtered from the acidic solution and hydrolyzed by stirring for 15 h under argon in a solution of 10 g of NaOH in 200 mL of water and 75 mL of ethanol. The resulting solution was acidified using 1 mM HCl, and the 1-adamantanethiol was separated via liquid−liquid extraction using chloroform and the acid solution, followed by rinsing with methylene chloride and hexanes. The resulting extracts were dried over anhydrous sodium sulfate and filtered, and the remaining solvent was removed by evaporation under Ar. ^{1}H NMR (three singlets): δ 2.03, 1.94, 1.67. ^{13}C NMR: δ 47.5, 43.1, 35.8, 30.1. Mp 100−102 °C. The proton and carbon NMRs were taken in $CDCl_3$ using a Bruker DPX-300 NMR.

2.2. Self-Assembled Monolayer Fabrication. All of the SAMs were assembled on Au{111} via solution deposition in sparged ethanol. Commercially available Au{111} on mica substrates (Molecular Imaging, Tempe, AZ) were flame annealed using a hydrogen flame immediately prior to deposition. Alkanethiolate SAMs were prepared by immersing the annealed substrates in a 1 mM ethanolic solution for 24 h, while 1-adamantanethiolate SAMs were made similarly from 10 mM solutions. Following deposition, each sample was rinsed in neat ethanol and blown dry with nitrogen twice.

Co-deposited SAMs were made from solutions containing both 1-adamantanethiol and alkanethiol in specified molar proportion to make 1 mM total thiolate solutions, and were then treated in the same manner as single-component SAMs. Alkanethiol-inserted SAMs were made by first fabricating a 1-adamantanethiolate SAM, confirming the presence of a well-ordered lattice using STM, and then immersing the sample into a 1 mM solution of alkanethiol for the specified time period. 1-Adamantanethiol-inserted alkanethiolate SAMs were made similarly, but instead used 10 mM 1-adamantanethiol solution. Subsequently, each sample was submitted to a rinse and dry cycle before returning them to the STM. All STM measurements were performed under ambient conditions using a custom beetle-style STM.[9,47]

To determine the lattice spacing of the 1-adamantanethiolate SAMs, the same tip was used to scan a SAM of known spacing (i.e., an alkanethiolate SAM) before and/or after scanning an 1-adamantanethi-

(32) Noh, J.; Hara, M. *Langmuir* **2002**, *18*, 1953.
(33) Charles, L. F. M.S. Thesis, The Pennsylvania State University, University Park, PA, 1999.
(34) Molina, L. M.; Hammer, B. *Chem. Phys. Lett.* **2002**, *360*, 264.
(35) Poirier, G. E. *Langmuir* **1997**, *13*, 2019.
(36) Nowacki, W. *Helv. Chim. Acta* **1945**, *28*, 1233.
(37) Nowacki, W.; Hedberg, K. W. *J. Am. Chem. Soc.* **1948**, *70*, 1497.
(38) Hu, Y.; Sinnott, S. B. *Surf. Sci.* **2003**, *526*, 230.
(39) Schleyer, P. v. R.; Donaldson, M. M. *J. Am. Chem. Soc.* **1960**, *82*, 4645.
(40) Schleyer, P. v. R.; Williams, J. E.; Blanchard, K. R. *J. Am. Chem. Soc.* **1970**, *92*, 2377.
(41) Shen, M.; Schaefer, H. F., III; Liang, C.; Lii, J.-H.; Allinger, N. L.; Schleyer, P. v. R. *J. Am. Chem. Soc.* **1992**, *114*, 497.
(42) Khullar, K. K.; Bauer, J. *J. Org. Chem.* **1971**, *36*, 3038.
(43) Mair, B. J.; Shamaiengar, M.; Krouskop, N. C.; Rossini, F. D. *Anal. Chem.* **1959**, *31*, 2082.
(44) Fujii, S.; Akiba, U.; Fujihira, M. *J. Am. Chem. Soc.* **2002**, *124*, 13629.
(45) Wakamatsu, S.; Fujii, S.; Akiba, U.; Fujihira, M. *Nanotechnology* **2003**, *14*, 258.
(46) Geigy, J. R. *Chem. Abstr.* **1964**, *60*, 9167.
(47) Mantooth, B. A. Ph.D. Thesis, The Pennsylvania State University, University Park, PA, 2004.

olate SAM. Alternatively, the lattice spacing was determined from a multicomponent SAM in which there were distinct ordered areas of 1-adamantanethiolate and alkanethiolate. In this way, the same tip was used to determine the lattice spacing of both simultaneously. In both cases, the measured spacing of the alkanethiolate SAM was used to calibrate the gain of the piezoelectric scanners and, thus, the measured lattice parameters. The 1-adamantanethiolate lattice spacing was measured from Fourier transforms of the images of the 1-adamantanethiolate lattice and was calibrated using the Fourier transform of the alkanethiolate lattice from the same or subsequent images. SAM corrugation was calibrated using the known height of the step edges of the Au{111} substrate in the same or subsequent images.

3. Results and Discussion

3.1. 1-Adamantanethiolate SAM Structure. Figure 1A shows two Au{111} terraces covered with a 1-adamantanethiolate SAM. A typical SAM of this type consists of very flat topography with depressions on the order of Au{111} substrate vacancy islands. With this resolution, it can be seen that 1-adamantanethiolate SAMs lack the protruding domain boundaries that are typical in alkanethiolate SAMs.[12,21,48,49]

Closer inspection at higher resolution (Figure 1B and C) shows individual molecules arranged in a hexagonal close-packed formation, and in addition to the substrate vacancy islands, there are apparent depressions of the molecular lattice of less than 0.5 Å. A Fourier transform of Figure 1C (shown in Figure 1D) shows a hexagonal lattice with the first- and second-order reciprocal lattice spots visible. However, these spots are not single points, but rather a collection of points the same distance from the center but slightly rotated. This distance in reciprocal space corresponds to a measured nearest neighbor distance of 6.9 ± 0.4 Å and a next nearest neighbor distance of 11.8 ± 0.4 Å. Measuring the angle spanned by the first-order spots (the angle formed by drawing a line from one end of the spot to center and back to the other end of the spot) in the Fourier transforms also shows that there are rotational domains of the hexagonal lattice with orientations as above.

With careful inspection, one should also observe that the rows of molecules shift direction slightly throughout the molecularly resolved images. It can be seen in Figure 2 that the apparent depressions mentioned above are domain boundaries separating different rotational domains. Five distinct domains (color coded and labeled in the bottom image of Figure 2) are observed, and their rotations with respect to one another are given in Table 1. The difference in orientation angles between domains A and E is small, and it is possible that these molecules belong to the same rotational domain. It should be noted that the exact rotation with respect to the substrate cannot be determined by imaging only the adlayer, although it is possible to estimate this rotation from straight step edges of the Au{111} substrate, which follow close-packed substrate directions.

Given the above observations, the most likely unit cell assignments are (7 × 7) with two rotationally equivalent unit cells of (7 × 7)*R*21.8° with respect to the Au{111}substrate, or the four rotationally equivalent unit cells ($\sqrt{91} \times \sqrt{91}$)*R*27° and ($\sqrt{91} \times \sqrt{91}$)*R*5.2° with respect to the Au{111} substrate, as shown schematically in Figure 3. It is also possible that the preferred orientation is some combination of each unit cell;

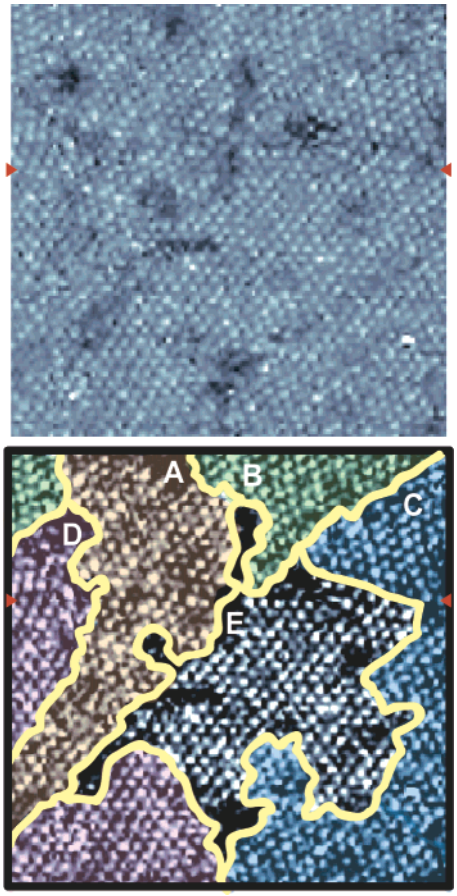

Figure 2. A scanning tunneling microscopy image of the domains of a 1-adamantanethiolate self-assembled monolayer on Au{111}. The same image is shown underneath with the domains highlighted and the contrast increased for clarity. The measured angles between the unit cells of the domains are given in Table 1 using the alphanumeric labels, indicated on the figure. A slight tip jump, marked by the red arrowheads, approximately two-thirds of the way up the image, gives the appearance of a change in rotation of the lattice, but instead the molecules are all uniformly shifted to the left across the image. The imaged area is 200 Å × 200 Å, sample bias 1.0 V, current 5.0 pA.

Table 1. Measured Angles between Each of the Observed Rotational Domains (Shown in Figure 2) of a 1-Adamantanethiolate Self-Assembled Monolayer[a]

	A	B	C	D	E
A		15° (CW)	7° (CW)	10° (CCW)	2° (CCW)
B	15° (CCW)		9° (CCW)	24° (CCW)	15° (CCW)
C	7° (CCW)	9° (CW)		15° (CCW)	8° (CCW)
D	9° (CW)	24° (CW)	15° (CW)		8° (CW)
E	2° (CW)	15° (CW)	8° (CW)	8° (CCW)	

[a] The direction of each angle is specified as clockwise (CW) or counterclockwise (CCW). All measured angles have an associated error of ±4°.

additional possibilities with nearest neighbor distances near 6.9 Å are not ruled out. Using a gold lattice spacing of 2.89 Å, a (7 × 7) unit cell has a lattice constant of 20.23 Å and has nine molecules per unit cell. Therefore, a (7 × 7) unit cell gives a nearest neighbor distance of 6.74 Å and a next nearest distance of 11.68 Å. A ($\sqrt{91} \times \sqrt{91}$) unit cell has a lattice constant of 27.57 Å with 16 molecules per unit cell, resulting in a nearest neighbor distance of 6.89 Å and a next nearest neighbor distance of 11.94 Å. All the calculated distances and angles for these unit cells are within the error of those measured. Note that these

(48) Delamarche, E.; Michel, B.; Gerber, C.; Anselmetti, D.; Guntherodt, H. J.; Wolf, H.; Ringsdorf, H. *Langmuir* **1994**, *10*, 2869.
(49) Sellers, H.; Ulman, A.; Shnidman, Y.; Eilers, J. E. *J. Am. Chem. Soc.* **1993**, *115*, 9389.

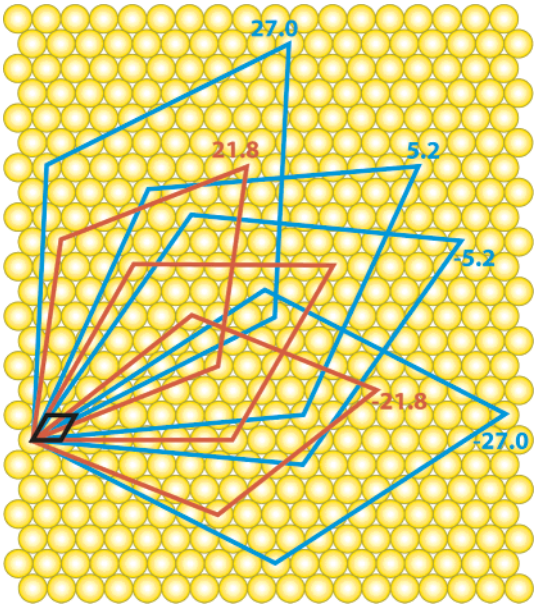

Figure 3. The possible unit cells for 1-adamantanethiolate SAMs on Au{111} with equivalent rotational unit cells shown for each. The (1 × 1) unit cell of the Au{111} substrate is shown in black, and the (7 × 7) and ($\sqrt{91}$ × $\sqrt{91}$) unit cells of the adlayer are drawn in red and blue, respectively.

Table 2. Measured Height Differences and Fractional Coverage for Solutions of Decanethiol and Octanethiol Inserted into Preformed 1-Adamantanethiolate SAMs[a]

Inserted Molecule	Apparent Height Difference	Coverage for Insertion Times 5 min	10 min	30 min
decanethiol	2.7 ± 0.5 Å	40%	55%	≥90%[b]
octanethiol	0.4 ± 0.2 Å	32%	43%	82%

[a] The fractional coverage was measured by counting the number of pixels with the same apparent height and dividing by the total available coverage. Substrate defects were not counted toward this total. The fractions were determined from images of the same size and resolution that cover only a single substrate terrace. [b] Due to the scarcity of 1-adamantanethiol molecules, the contrast of the SAM was not high enough to determine an exact fraction, but it was apparent from the images that the SAMs were predominately composed of decanethiolate.

lattice spacings are significantly larger than those found in alkanethiolate SAMs.

The measured apparent height differences between 1-adamantanethiol and two alkanethiols with different chain lengths are given in Table 2. 1-Adamantanethiolate is estimated to stand 7.9 Å off the surface, including the 2.36 Å sulfur−gold bond.[7] Using 1.1 Å per methylene unit length for the alkanethiolate matrices, the measured apparent height in STM images of the 1-adamantanethiolate SAM is 8.3 ± 0.5 Å. As discussed below, because of steric hindrance, there is likely little tilting of the 1-adamantanethiolate molecules with respect to the gold surface, further supporting the idea that the different domains are due to changes in rotation of the unit cell.

3.2. Displacement Studies. The regularity and lack of large defect sites as well as the minimal internal conformational relaxation make 1-adamantanethiolate SAMs appealing matrices for molecular electronics. Insertion of molecules with electronic function into an existing 1-adamantanethiolate SAM by previously described methods[3] was attempted for several molecules, but resulted in coverages of the inserted species that were too high to allow single inserted molecules to be probed when conditions that had been used previously for inserting molecules in alkanethiolate matrices were mimicked.[1,3,50,51] Further investigations of this phenomenon were performed inserting 1 mM decanethiol, octanethiol, or hexanethiol into preformed 1-adamantanethiolate SAMs for a variety of time scales. Table 2 shows the fraction of inserted decanethiolate or octanethiolate in images of inserted 1-adamantanethiolate SAMs for three insertion times. The fractional coverage was measured from representative images of each sample. The images were scaled to have high contrast between the two molecules on the surface based on apparent height differences. The pixel fraction of the image covered by each apparent height type (and therefore domains of each molecule) was calculated and then divided by the total lattice coverage. Defects in the substrates were not included. All of the coverages were calculated from images 500 Å × 500 Å in size that include only one substrate terrace. The associated error for all the percentages shown is ±2%.

For insertion times of less than 1 min in a 1 mM decanethiol solution, we found spotty coverage of which only a few percent of the resulting SAM was composed of decanethiolate. After 5 min, patches of decanethiolate covered ~40% of the surface, and with longer insertion times, the coverage increase radially outward from the patches until the entire 1-adamantanethiolate SAM was replaced by decanethiolate (more than 30 min). These patches were ordered domains of decanethiolate (see Figure 4A and B), and it was possible to resolve the lattice of both the 1-adamantanethiolate and decanethiolate portions simultaneously (although this is significantly easier when the apparent heights of the two components are similar).

When inserting 1 mM octanethiolate into the 1-adamantanethiol SAMs, the same process occured. Spotty coverage primarily around the defects was observed for low insertion times, with increased coverage extending out from the insertion points for longer time scales. Slightly lower fractions (although not dramatically different) were observed on the same time scales as those for decanethiolate insertions. This may correlate to the difference in hydrocarbon tail lengths and to the difference in the speed of ordering due to larger intermolecular van der Waals forces between the decanethiol relative to octanethiol molecules.[12,14,21,30]

Insertion of 1 mM hexanethiol into 1-adamantanethiolate SAMs also resulted in a mixed SAM with both lattices apparent. However, instead of the SAM being composed of mostly 1-adamantanethiolate lattice with patches of hexanethiolate (as seen for the other alkanethiol insertions), in addition to small hexanethiolate patches, there were also striped regions and regions of disorder (see Figure 5 top). The regions of disorder were likely areas of mixed, unordered 1-adamantanethiolate and hexanethiolate molecules. The stripes were observed in three orientations, rotated 120° from each other. As shown in Figure 6, each stripe set consists of a row of smaller molecules spaced 5.1 ± 0.5 Å apart (row A in Figures 5 and 6), then two rows of larger molecules spaced 11 ± 1.0 Å apart (rows B and C), followed by another row of molecules that appear less protruding in the STM images (row D). The molecular spacings of row A and rows B and C correlate well to the nearest neighbor distance of an alkanethiolate lattice and the previously discussed

(50) Cygan, M. T.; Dunbar, T. D.; Arnold, J. J.; Bumm, L. A.; Shedlock, N. F.; Burgin, T. P.; Jones, L.; Allara, D. L.; Tour, J. M.; Weiss, P. S. *J. Am. Chem. Soc.* **1998**, *120*, 2721.
(51) Dameron, A. A.; Ciszek, J. W.; Tour, J. M.; Weiss, P. S. *J. Phys. Chem. B* **2004**, *108*, 16761.

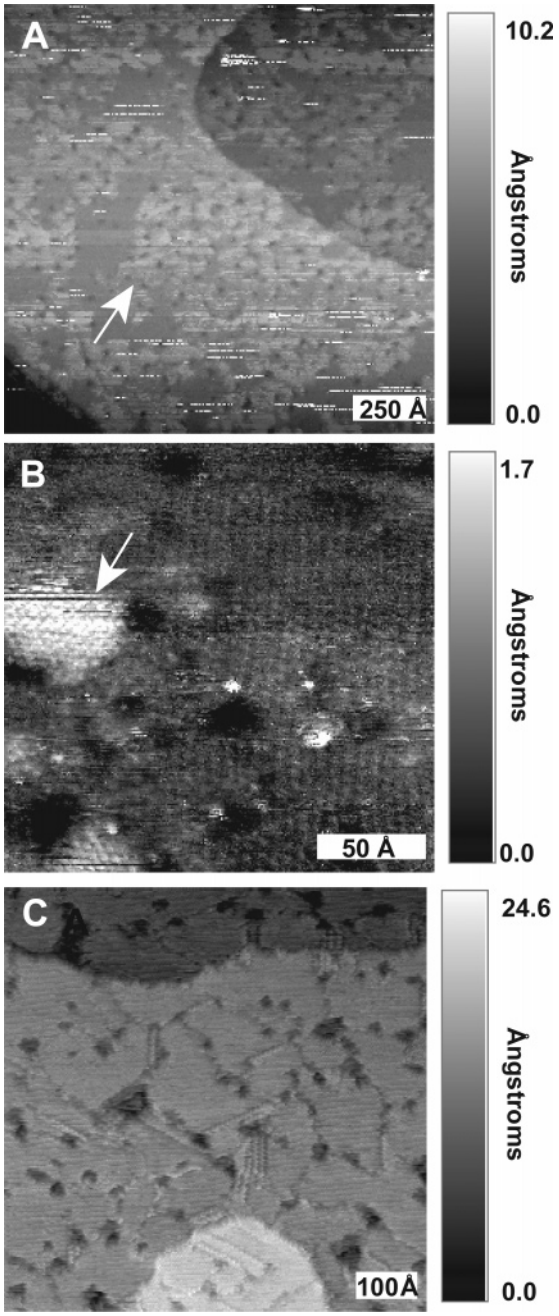

Figure 4. (A and B) Scanning tunneling microscopy images of 1-adamantanethiolate SAMs with decanethiol inserted for 10 min. The decanethiolate protrudes beyond the 1-adamantanethiolate in ordered patches, indicated by the arrows. (A) 1500 Å × 1500 Å, sample bias 1.0 V, current 1.0 pA; (B) 200 Å × 200 Å, sample bias 1.0 V, current 2.0 pA. (C) A decanethiolate SAM with 1-adamantanethiol inserted for 30 min. No regions of remaining 1-adamantanethiolate are observed; 700 Å × 700 Å, sample bias 1.0 V, current 2.0 pA.

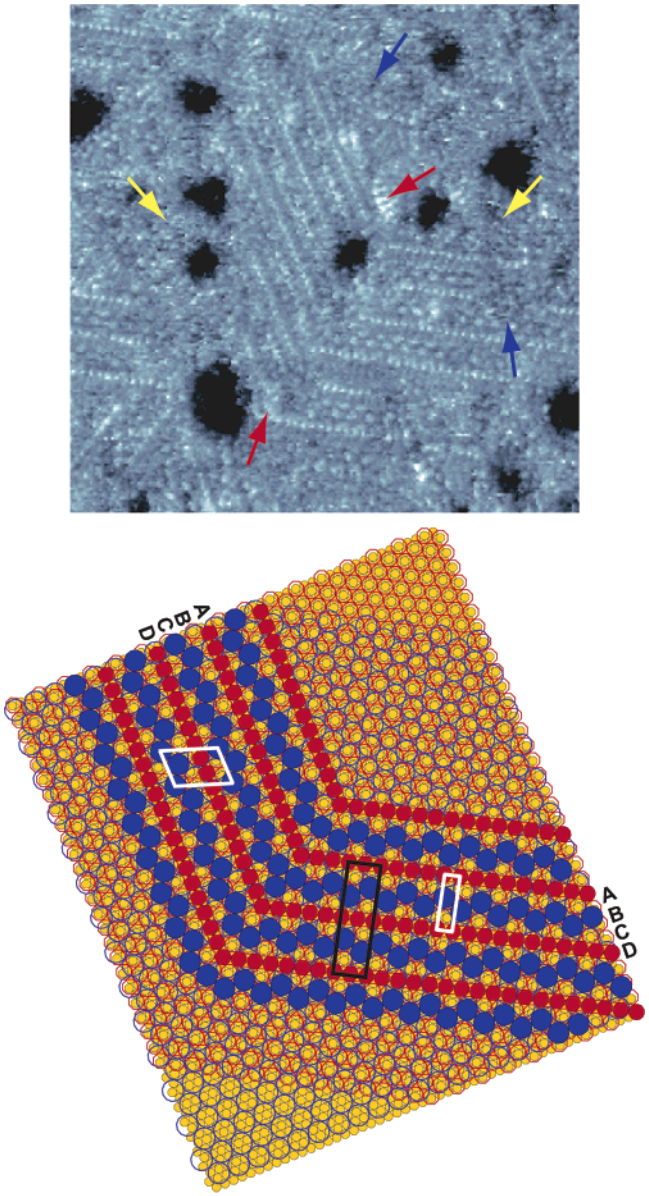

Figure 5. (Top) A scanning tunneling microscopy image of an 1-adamantanethiolate self-assembled monolayer on Au{111} that was immersed for 30 min in a 1 mM hexanethiol solution. The red, blue, and yellow arrows indicate patches of ordered hexanethiolate, regions of ordered 1-adamantanethiolate, and regions of disorder, respectively; 300 Å × 300 Å, sample bias 1 V, current 4.0 pA. (Bottom) A model of the 1-adamantanethiolate and hexanethiolate stripes on Au{111} using a (7 × 7) unit cell for 1-adamantanethiolate SAM and a $(\sqrt{3} \times \sqrt{3})R30°$ unit cell for hexanethiolate SAM. The white boxes indicate the $(4 \times 4\sqrt{7/3})R30°$ (left) and $(6 \times \sqrt{3})$ (right) subunit cells of the striped 1-adamantanethiolate lattice and hexanethiolate lattice, respectively. The black box indicates the $(13 \times 2\sqrt{3})$ unit cell of the hexanethiolate and adamantanethiolate stripes together.

measured next nearest neighbor distance of an 1-adamantanethiolate lattice, respectively. On the basis of these spacings and the relative sizes of the two molecules, the molecules of rows A and D are assigned as hexanethiolate and the molecules in the middle rows B and C as 1-adamantanethiolate. Seen most clearly in the inset of Figure 6, the alkanethiolate molecules in row A are positioned directly across from those in row D, while the 1-adamantanethiolate molecules in row B are staggered with the molecules in row C (i.e., the molecules in row B are nearest neighbors of the molecules in row C). Furthermore the 1-adamantanethiolate rows in a stripe set are staggered with respect to the equivalent rows in a neighboring stripe set. Upon closer inspection of the hexanethiolate rows, additional hexanethiolate molecules are observed. The arrow in the inset of Figure 6 shows the apparent pairing of two hexanethiolate molecules in row D with a third molecule in the nearest neighbor position between rows D and C. Other hexanethiolate molecules were observed along row D as well as above row A. The extra molecules did not occur all the way along the row and did not appear uniformly

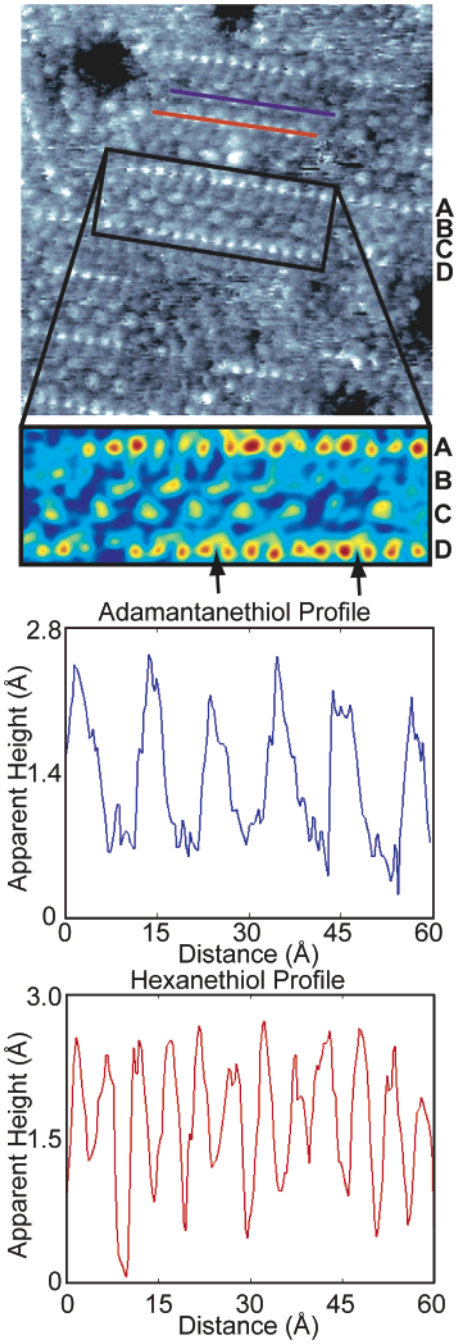

Figure 6. At the top is a scanning tunneling microscopy image of a 1-adamantanethiolate self-assembled monolayer on Au{111} immersed for 30 min in a 1 mM hexanethiol solution. The inset shows a detailed single stripe set with the 1-adamantanethiolate molecules zig-zagging on the interior, displayed in yellow (rows B and C), and the hexanethiolate molecules lined up on the exterior, displayed in red (rows A and D). The black arrows indicate example additional hexanethiolate molecules close to the nearest neighbor position of the hexanethiolate molecules in row D; 150 Å × 150 Å, sample bias 1 V, current 4.0 pA (top). Profiles of the adamantanethiolate and hexanethiolate rows (lines on the STM image in blue and red, respectively) are shown below.

spaced, nor were they uniformly the same apparent height, possibly indicating strained conformations.

The measured distance between the hexanethiolate rows (A−D) is 22 ± 2 Å. The measured distance between a hexanethiolate and the nearest 1-adamantanethiolate (A−B) row is 8 ± 2 Å and between a hexanethiolate and the farthest 1-adamantanethiolate row (A−C) is 12 ± 2 Å. Therefore, the measured distance between two 1-adamantanethiolate rows (B−C) is approximately 4 Å; this is possible because of the staggered arrangement of the molecules.

As shown in Figure 5, it is possible to model the striped regions using a $(\sqrt{3} \times \sqrt{3})R30°$ unit cell for hexanethiolate and a (7×7) unit cell for 1-adamantanethiolate with respect to the Au{111} surface. Using the orientation of the hexanethiolate lattice with respect to a substrate step edge (not shown), it is possible to determine the orientation of the Au{111} lattice and, therefore, the associated orientation to the 1-adamantanethiolate lattice. Given the above observation that the rows of hexanethiolate molecules are aligned with one another and the 1-adamantanethiolate molecules are not, it is determined that two hexanethiolate rows must be an even integer apart (i.e., every second, fourth, sixth, etc. row), while the 1-adamantanethiolate rows must be an odd integer apart (i.e., first (nearest neighbor), third, etc. row). From the measured row spacings, the most likely orientation is the one shown in the model, with the hexanethiolate rows repeating every four rows and the 1-adamantanethiolate rows paired and repeating every three rows. In this orientation, the hexanethiolate molecules are arranged in a $(6 \times \sqrt{3})$ unit subcell, and the adamantanethiolate molecules form a $(4 \times 4\sqrt{7/3})R30°$ unit subcell with respect to the Au{111}. Both molecules together form a $(13 \times 2\sqrt{3})$ unit cell (shown in black in Figure 5). The model also demonstrates that there is enough room for an extra hexanethiolate molecule near the hexanethiolate nearest neighbor positions, although not always at the preferred nearest neighbor alkanethiolate spacing, explaining the strained appearance.

When 1-adamantanethiol is inserted from a 10 mM solution into alkanethiolate SAMs, very little displacement is observed. As shown in Figure 4C, the adamantanethiol molecules insert sparsely around the defects of the decanethiolate SAMs, but they do not displace the existing molecular lattice. Insertion times of 1-adamantanethiol up to 24 h still result in nearly pure alkanethiolate SAMs.

Co-adsorption studies were also performed in which deposition times of 24 h were used to make SAMs from two-component solutions in which the relative molar ratio of decanethiol to 1-adamantanethiol was varied. The type of SAM and the resulting order were monitored, and examples are shown in Figure 7. An ordered SAM of decanethiolate results when the solution consisted of molar ratios of less than 90:10 1-adamantanethiol:decanethiol (Figure 7A). However, the decanethiolate SAMs have more and smaller domains than a typical decanethiolate SAM made with a 24 h deposition time and are often disordered at domain boundaries. For molar percentages of 10% decanethiol in solution, a disordered SAM of both decanethiolate and 1-adamantanethiolate results (see Figure 7B). For molar percentages of less than 5% decanethiol, an ordered SAM of 1-adamantanethiolate results (Figure 7C) with small clusters of decanethiolate molecules randomly dispersed throughout the SAM, similar to the samples seen for the insertion studies with low insertion times.

Figure 8 schematically shows possible explanations for the susceptibility of 1-adamantanethiolate SAMs to displacement. SAMs of *n*-alkanethiolates are stabilized considerably by the presence of intermolecular van der Waals forces and tilt so as to maximize these chain−chain attractive interactions.[12,21,30,48,49] The 1-adamantanethiolate SAMs have substantially lower van

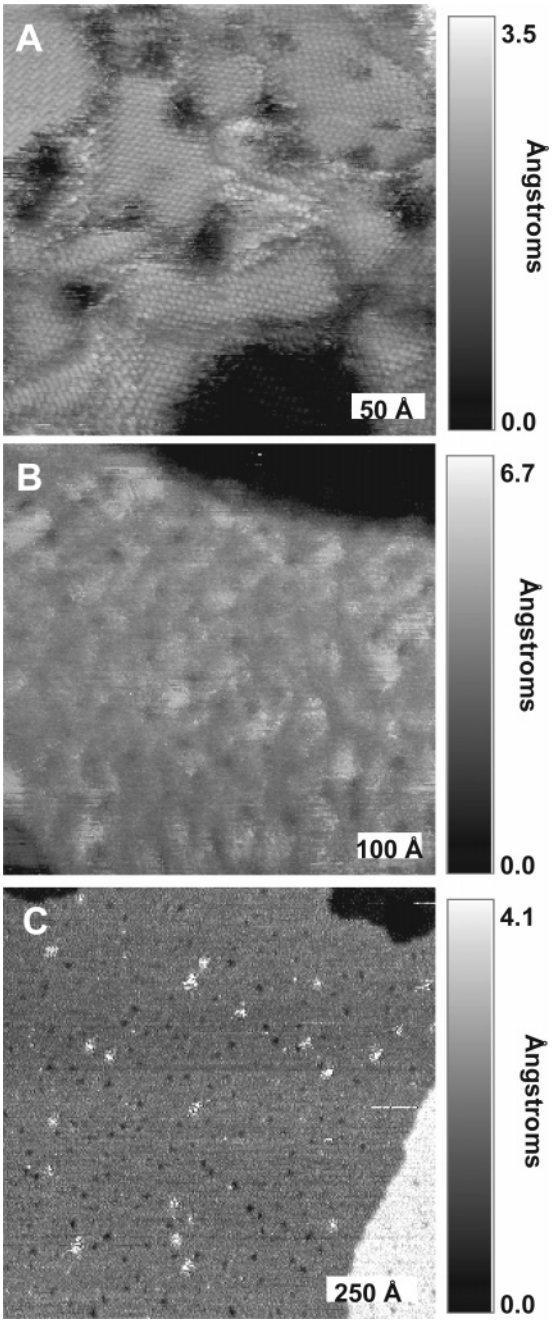

Figure 7. Scanning tunneling microscopy images of co-deposited 1-adamantanethiolate and decanethiolate SAMs: (A) A 50:50 (1-adamantanethiol:decanethiol) solution molar ratio results in a decanethiolate SAM; 300 Å × 300 Å, sample bias 1.0 V, current 5.0 pA. (B) A 90:10 solution molar ratio results in a disorder SAM containing both 1-adamantanethiolate and decanethiolate; 700 Å × 700 Å, sample bias 1.0 V, current 2.0 pA. (C) A 99:1 solution molar ratio results in an ordered 1-adamantanethiolate SAM with decanethiolate clusters (the small protrusions apparent in the image); 1200 Å × 1200 Å, sample bias 1.0 V, current 7.0 pA.

der Waals forces than those that strengthen and order *n*-alkanethiolate SAMs because of the larger distance between the molecules, the limited intermolecular contact, and the insignificant conformational relaxation.[17,20,28] Also, due to the length of the thiolate tether to the gold and the bulky shape of the molecule, it is unlikely that the adamantanethiolate molecules could be significantly tilted from normal to the gold surface without straining the thiolate−gold bond. We expect, based on molecular models, that the lower hydrogens on the adamantane

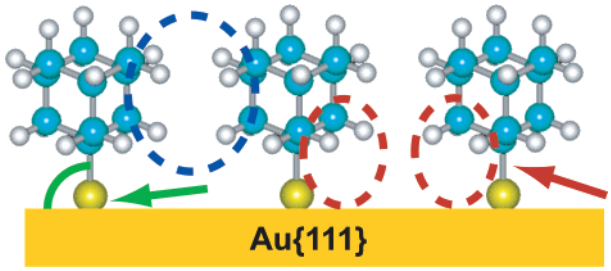

Figure 8. Proposed schematic of the propensity for 1-adamantanethiolate displacement. (1) Compared to alkanethiol SAMs, there are much reduced van der Waals interactions between the neighboring molecules because of the distance between them (blue). (2) The sulfur−gold bond is not in its most favorable conformation (green). (3) The steric repulsion from the lower hydrogens cause the bonds tethering the molecules to the gold to extend (red).

cage experience steric repulsion from the gold surface, which may further weaken the bond to the surface. The substrate access between molecules, the lack of substantial intermolecular stabilization, and the weakened Au−molecule bonds all make adamantanethiolate susceptible to displacement.

The exact mechanism for displacement by alkanethiol molecules is unknown. One possibility is that the slimmer alkanethiol molecules first insert in and around the defects in the 1-adamantanethiolate SAM. The presence of the first alkanethiolate molecules then causes instability in the surrounding 1-adamantanethiolate molecules, causing those to be displaced and allowing further insertion of alkanethiolate molecules. In this way, the alkanethiolate islands grow outward from defects in the 1-adamantanethiolate SAMs, as observed.

The reason for the striping of inserted hexanethiolate molecules rather than the patches observed for octanethiolate and decanethiolate is most likely a result of lowered van der Waals forces between hexanethiol molecules because of the shorter alkyl tails. With decreased tail length, the direction of tilt of the alkanethiol molecules shifts toward the nearest neighbor direction because of a balance between the amount of molecular strain and the degree of molecular packing order, both of which are influenced by the hydrocarbon tail length.[52] Alkanethiolate molecules with alkyl tail lengths below eight carbons demonstrate an affinity for the striped phase in pure SAMs, especially for shorter deposition times.[18,53−57] Under low surface coverage conditions, it has been demonstrated that alkanethiolate molecules form a $(p \times \sqrt{3})$ rectangular unit mesh with three equivalent orientations.[19] Furthermore, Noh et al. have shown that recrystallization of a disordered hexanethiolate SAM results in a $(6 \times \sqrt{3})$ structure with alternating missing rows in the nearest neighbor direction.[54]

It is postulated that the inserted hexanethiolate molecules assemble in linear stripes rather than growing radially in patches because of the combination of lowered van der Waals molecular interactions (related to the decreased alkyl tail length) and anisotropy created by the insertion of a tilted molecule. Because of the lowered van der Waals interactions, there is no driving force for the hexanethiol molecules to insert near existing

(52) Fenter, P.; Eberhardt, A.; Liang, K. S.; Eisenberger, P. *J. Chem. Phys.* **1997**, *106*, 1600.
(53) Noh, J.; Hara, M. *Mol. Cryst. Liq. Cryst.* **2000**, *349*, 223.
(54) Noh, J.; Hara, M. *Langmuir* **2001**, *17*, 7280.
(55) Noh, J.; Nakajima, K.; Hara, M.; Sasabe, H.; Knoll, W.; Lee, H. *Korea Polym. J.* **1998**, *6*, 307.
(56) Poirier, G. E. *Langmuir* **1999**, *15*, 1167.
(57) Poirier, G. E.; Tarlov, M. J. *J. Phys. Chem.* **1995**, *99*, 10966.

hexanethiolate molecules; however, should one insert near an existing hexanethiolate molecule, the alkyl tails tilt so as to maximize interactions, creating linear anisotropy. This anisotropy causes strain of the adamantanethiolate molecules in that direction, thereby enabling the next hexanethiol molecules to displace the neighboring strained adamantanethiolate molecules.

It is unclear if there is a preferred insertion direction with respect to gold and/or if one 1-adamantanethiolate molecular site is more likely to be displaced than another. Further displacement studies altering the tether length of the adamantanethiol molecules in addition to changing the structure of the molecules inserted into the 1-adamantanethiol SAMs are ongoing.

4. Conclusions and Prospects

Novel 1-adamantanethiolate SAMs with fewer defects than alkanethiolate SAMs have been fabricated and studied with STM. A measured nearest neighbor distance of 6.9 ± 0.4 Å and five rotational domains of the lattice are observed, implying some combination of (7×7), $(7 \times 7)R21.8°$, $(\sqrt{91} \times \sqrt{91})R27°$, or $(\sqrt{91} \times \sqrt{91})R5.2°$ unit cells. The bonding of the adamantanethiolate SAMs to the Au{111} was explored by monitoring both the displacement of the 1-adamantanethiolate molecules upon insertion of alkanethiol molecules into the matrix and the co-deposition of both species from solution. It was found that 1-adamantanethiolate molecules are easily displaced by alkanethiolate molecules, and this eventually leads to complete replacement of the 1-adamantanethiolate SAM. We propose that displacement of 1-adamantanethiolate SAMs can be exploited for use in patterned SAMs without risk of disturbing the patterned features, and that these transient SAMs can be used as temporary layers in soft lithography for protection of volatile or reactive surfaces, and can then be easily removed prior to initiation of the next fabrication step. We are currently attempting to exploit displacement in this manner.

Acknowledgment. The authors thank Dr. P. A. Lewis, N. Santagata, and Prof. K. F. Kelly for their analytical assistance, R. K. Smith for synthetic aid, B. A. Mantooth for hardware and software support, and Dr. E. C. H. Sykes and Dr. L. C. Fernández-Torres for helpful discussions. The Air Force Office of Scientific Research, Army Research Office, Defense Advanced Research Projects Agency, National Science Foundation, Office of Naval Research, and Semiconductor Research Corporation are gratefully acknowledged for their support.

JA042621O